Synthetic, Structural, and Theoretical Studies on the Electron-Deficient Cubanes $(RC_5H_4)_4Ti_4S_4$, $(RC_5H_4)_4V_4S_4$, and $[(RC_5H_4)_4V_4S_4]^+$

James Darkwa,[1a] John R. Lockemeyer,[1a] Peter D. W. Boyd,*[1b] Thomas B. Rauchfuss,*[1a] and Arnold L. Rheingold*[1c]

Contribution from the School of Chemical Sciences, University of Illinois, Urbana, Illinois 61801, Department of Chemistry, University of Auckland, Auckland, New Zealand, and Department of Chemistry, University of Delaware, Newark, Delaware 19711. *Received May 4, 1987*

Abstract: Treatment of $(MeCp)_2V_2S_4$ with PBu_3 gives the electron-deficient (56e) cubane $(MeCp)_4V_4S_4$ (**1**). Desulfurization of a 1:1 mixture of $(MeCp)_2V_2S_4$ and $Cp_2V_2S_4$ gave a mixture of ring-substituted cubanes $(MeCp)_{4-x}Cp_xV_4S_4$ (x = 1-4) while $(MeCp)_2V_2S_4$ and Cp_2V react to give exclusively $(MeCp)_2Cp_2V_4S_4$. Compound **1** has a triplet (S = 1) ground state, exhibits Curie-Weiss magnetic behavior, and has a well-resolved isotropically shifted ^1H NMR spectrum. Cyclic voltammetry (vs Ag/AgCl) established the following redox series: $\mathbf{1}^+/\mathbf{1}$ (772 mV), $\mathbf{1}/\mathbf{1}^-$ (176 mV), and $\mathbf{1}^-/\mathbf{1}^{2-}$ (-1281 mV). The salt $[\mathbf{1}](BF_4)$ was prepared by the reaction of **1** and Ph_3CBF_4. The diamagnetic 52e cubanes $(RCp)_4Ti_4S_4$ (R = Me (**2**), i-Pr) were prepared from $(RCp)TiCl_2(THF)_x$ and $(Me_3Si)_2S$. The compounds **1**, $[\mathbf{1}](BF_4)$, and **2** were characterized by single-crystal X-ray diffraction. Compound **1** crystallized in the cubic space group $P\bar{4}3n$ with a = 16.551 (3) Å with Z = 6; 671 unique reflections were processed to a final $R(F)$ = 5.31 ($R_w(F)$ = 5.80). Compound $[\mathbf{1}](BF_4)$ crystallized in the tetragonal space group $I\bar{4}$ with a = 10.600 (3) Å and c = 12.600 (3) Å with Z = 2; 463 unique reflections were processed to a final R = 6.40 ($R_w(F)$ = 6.55). Compound **2** crystallized in the orthorhombic space group $Cmca$ with a = 1.412 (5), b = 17.293 (6), c = 24.503 (9) Å with Z = 8; 558 unique reflections were processed to give R = 10.5 ($R_w(F)$ = 12.6). **1** and $[\mathbf{1}]^+$ are extremely similar structurally; no bond distances differ by more than 0.03 Å. The structure of **2** revealed two sets of Ti-Ti distances, four distances of 3.00 Å and two of 2.93 Å. Electronic structure calculations of $Cp_4V_4S_4$ and $[Cp_4V_4S_4]^+$ were performed by the scattered wave-Xα method. The ground-state configuration for the $Cp_4V_4S_4$ metal bonding orbitals is $a_1^2e^4t_2^2$. The t_2 orbital is predicted to be nonbonding, consistent with the structural results. The bonding in **1**, $\mathbf{1}^+$, and **2** is discussed in light of recent results from other laboratories.

Cubane clusters of the formula $(L_nM)_4E_4$ are one of the major classes of tetrametallic compounds. Their structures consist of interpenetrating tetrahedra of main-group atoms (E) and metals where the latter are bound to terminal ligands (L). Isolated cubane subunits occur in living systems[2] and in solid-state polymers.[3] A particularly extensive class of molecular cubanes feature M_4S_4 cores and cyclopentadienyl (Cp) coligands.[4] These $Cp_4M_4S_4$ clusters are in many ways electronically and structurally representative of a large family of low-spin $(L_nM)_4E_4$ clusters where L_n = $(CO)_3$, arene, NO, $(CN)_3$, $(H_3O)_3$, etc., and E = chalcogen or pnictogen.

For low-spin $(ML_n)_4E_4$ cubanes the maximum valence electron count for the M_4 units is 72. The value arises from complete occupation of the nine valence orbitals on each metal. Examples of 72e cubanes are $Cp_4Co_4S_4$[5] and $Fe_4S_4(CO)_{12}$.[6] Both have tetrahedral M_4 cores with long, nonbonding metal-metal distances. At the other extreme, 60e clusters also have highly symmetrical tetrahedral M_4 cores but with short intermetallic distances indicative of a net metal-metal bond order of 6. Premier examples of 60e cubanes are $(i\text{-PrCp})_4Mo_4S_4$[7] and $Fe_4S_4(NO)_4$.[8] Many cubanes are known with valence electron counts between 60 and 72.

The expanded scope of early transition metal chemistry has finally permitted investigations of $Cp_4M_4S_4$ cubanes with fewer than the 60e. Incremental decreases in cubane electron count have been achieved recently beginning with $Cp_4Cr_3VS_4$ (59e),[9] (i-$PrCp)_4Mo_4S_4^{+/2+}$ (59e, 58e),[7] and $Cp_4V_4S_4$ (56e).[10-12] Additionally, heterometallic cubanes of the formula $Cp_2V_2M_2(NO)_2S_4$ where M_2 = Fe_2 (58e), FeCo (59e), Co_2 (60e), and Ni_2 (62e) have been prepared and structurally characterized.[13] This paper summarizes our work on cubanes with fewer than 56e including the exceptionally electron-deficient species $(i\text{-PrCp})_4Ti_4S_4$ (52e).

Using a qualitative molecular orbital model, Dahl and coworkers[8] have successfully explained many of the structural variations in $Cp_4M_4S_4$ clusters with valence electron counts ≥60e. In this model, the strong metal-ligand interactions (i.e., M-S and M-Cp) are energetically well separated from the higher lying metal-based orbitals. These metal-based orbitals are primarily d orbital in character and may be subdivided into three energetically distinct groups: (1) six orbitals that correspond to direct metal-metal bonding ($a_1 + e + t_2$), (2) eight nonbonding (with respect to the other metals) orbitals ($e + t_1 + t_2$), and (3) six metal-metal antibonding orbitals ($t_1 + t_2$). The nonbonding set of metal orbitals are proposed to be destabilized (relative to the metal-metal bonding and antibonding levels) by antibonding interactions with the ligand orbitals.[5,14] It has been suggested[15] (and disputed[4]) that the relative energies of some of the metal-metal bonding orbitals are also strongly modulated by their interactions with the lone pairs localized on sulfur (of $a_1 + t_2$

(1) (a) University of Illinois. (b) University of Auckland. (c) University of Delaware.
(2) Averill, B. A.; Orme-Johnson, W. H. In *Metal Ions in Biological Systems*; Sigel, H., Ed.; Dekker: New York, 1978; Vol. VII.
(3) Hiebl, K.; Sienko, M. J.; Rogel, P. *J. Less-Common Met.* **1981**, *82*, 21.
(4) Williams, P. D.; Curtis, D. *Inorg. Chem.* **1986**, *25*, 4562.
(5) Simon, G. L.; Dahl, L. F. *J. Am. Chem. Soc.* **1973**, *95*, 2164.
(6) Nelson, L. F.; Lo, F. Y.-K.; Rae, A. D.; Dahl, L. F. *J. Organomet. Chem.* **1982**, *225*, 309.
(7) Bandy, J. A.; Davies, C. E.; Green, J. C.; Green, M. L. H.; Prout, K. Rodgers, D. P. S. *J. Chem. Soc., Chem. Commun.* **1983**, 1395.
(8) Cho, C. T.-W.; Lo, F. Y.-K.; Dahl, L. F. *J. Am. Chem. Soc.* **1982**, *104*, 3409.
(9) Pasynskii, A. A.; Eremenko, I. L.; Orazsakhatov, B.; Kalinnikov, V. T.; Aleksandrov, G. G.; Struchkov, Yu. T. *J. Organomet. Chem.* **1981**, *216*, 211.
(10) Bolinger, C. M. Ph.D. Thesis, University of Illinois at Urbana—Champaign, 1984.
(11) Eremenko, I. L.; Pasynskii, A. A.; Katugin, A. S.; Ellert, O. G.; Suklover, V. E.; Struchkov, Y. T. *Bull. Acad. Sci. USSR, Div. Chem. Sci. (Engl. Transl.)* **1983**, 1531.
(12) Bolinger, C. M.; Darkwa, J.; Gammie, G.; Gammon, S. E.; Lyding, J. W.; Rauchfuss, T. B.; Wilson, S. R. *Organometallics* **1986**, *5*, 2386.
(13) Rauchfuss, T. B.; Weatherill, T. D.; Wilson, S. R.; Zebrowksi, J. P. *J. Am. Chem. Soc.* **1983**, *105*, 6508. Weatherill, T. D. Ph.D. Thesis, University of Illinois at Urbana—Champaign, 1985.
(14) Trinh-Toan; Fehlhammer, W. P.; Dahl, L. F. *J. Am. Chem. Soc.* **1977**, *99*, 402. Trinh-Toan; Teo, B. K.; Ferguson, J. A.; Meyer, T. J.; Dahl, L. F. *J. Am. Chem. Soc.* **1977**, *99*, 408.
(15) Bottomley, F.; Green, F. *Inorg. Chem.* **1982**, *21*, 4120.

0002-7863/88/1510-0141$01.50/0

symmetry) and by back-bonding from the C_5H_5 group (e + t_1 + t_2 orbitals).[16] The highly electron-deficient clusters described in this work provide an opportunity to investigate the metal–metal bonding in this class of compounds. Additionally, we describe new synthetic routes to these cubane clusters.

Results

Synthesis of V_4S_4 and Ti_4S_4 Cubanes. The compound $(MeCp)_4V_4S_4$ (**1**) was prepared in 45% yield by treating $(MeCp)_2V_2S_4$[17] with PBu_3. The analogous reaction with $Cp_2V_2S_4$ afforded $Cp_4V_4S_4$, which is noticeably less soluble than the methylcyclopentadienyl species. The $(RCp)_4V_4S_4$ clusters are sublimable and are easily obtained as microcrystalline solids. They exhibit strong molecular ion peaks in their electron-impact mass spectra. The ^1H NMR spectra are strongly shifted from the expected diamagnetic positions (Table I). Compound **1** has a triplet ($S = 1$) ground state as established by its room-temperature magnetic moments (2.68 μ_B at 300 K) and the linearity of the $1/\chi$ vs T plot.[10] Compound **1** has recently been studied by Russian workers who prepared it from $(MeCp)_2V$ and *t*-BuSH.[11] Analogues of **1** can also be prepared via the reaction of Cp_2V and $(MeCp)_2V_2S_4$, which gives high yields of $Cp_2(MeCp)_2V_4S_4$. Attempts to prepare the 1:1 adduct $Cp_2V{\cdot}(MeCp)_2V_2S_4$ were unsuccessful. $Cp_2(MeCp)_2V_4S_4$ was definitively characterized by its isotropically shifted ^1H NMR spectrum as well as by mass spectrometry.

Also formed in the desulfurization of $(MeCp)_2V_2S_4$ is $(MeCp)_5V_5S_6$.[12] The formation of both V_4 and V_5 clusters suggests that the PBu_3 reaction involves the formation of *mono*vanadium intermediates. Further evidence along these lines is that treatment of an equimolar mixture of $Cp_2V_2S_4$ and $(MeCp)_2V_2S_4$ with PBu_3 results in the formation of significant amounts of all five cubanes $(MeCp)_{4-x}Cp_xV_4S_4$. A series of control experiments show that, once formed, these V_4S_4 cubanes do not undergo exchange with other $(RCp)VS_n$ moieties (Scheme I).

Scheme I

$$(MeCp)_2V_2S_4 \xrightarrow[-SPBu_3]{+PBu_3} (MeCp)_4V_4S_4 + (MeCp)_5V_5S_6$$

$$Cp_2V_2S_4 \xrightarrow[-SPBu_3]{PBu_3} Cp_4V_4S_4 + Cp_5V_5S_6$$

$$(MeCp)_2V_2S_4 + Cp_2V_2S_4 \xrightarrow[-SPBu_3]{PBu_3} (MeCp)_{4-x}Cp_xV_4S_4$$

$$Cp_4V_4S_4 + (MeCp)_4V_4S_4 \rightarrow NR$$

$$Cp_2V_2S_4 + (MeCp)_4V_4S_4 \rightarrow NR$$

$$Cp_2V_2S_4 + (MeCp)_4V_4S_4 \xrightarrow[SPBu_3]{PBu_3} Cp_4V_4S_4 + (MeCp)_4V_4S_4$$

$$(MeCp)_2V_2S_4 + 2Cp_2V \xrightarrow{-2Cp} (MeCp)_2Cp_2V_4S_4$$

A number of routes to $(RCp)_4Ti_4S_4$ were examined,[18] particularly those starting from solvates of $(RCp)TiCl_2$ (R = H, Me, *i*-Pr). THF solutions of the latter react with $(Me_3Si)_2S$ to give moderate yields of $(RCp)_4Ti_4S_4$ isolated as air-sensitive brown crystals (eq 1). ^1H NMR spectroscopy showed that these Ti_4S_4

$$4(RCp)TiCl_2(THF)_2 + 4(Me_3Si)_2S \rightarrow (RCp)_4Ti_4S_4 + 8Me_3SiCl \quad (1)$$

R = H, CH_3 (**2**), *i*-Pr

cubanes are diamagnetic. Unlike the V_4S_4 cubanes, the Ti_4S_4 clusters are not appreciably volatile and are highly reactive toward protic reagents such as alcohols. The compound $(MeCp)_4Ti_4S_4$ (**2**) was further characterized by X-ray diffraction.

Table I. ^1H NMR Data for Cubane Clusters

compound	^1H NMR ($CDCl_3$),[a] ppm	fwhh,[b] Hz
$(MeCp)_4V_4S_4$	59.2 (2 H, m)	72
	58.4 (2 H, m)	72
	7.6 (3 H, s)	14
$Cp_2(MeCp)_2V_4S_4$	59.4 (2 H, m)	73
	59.2 (2 H, m)	73
	53.6 (5 H, s)	60
	7.5 (3 H, s)	14
$[(MeCp)_4V_4S_4](BF_4)$	28.6 (2 H, m)	20
	28.2 (2 H, m)	20
	2.9 (3 H, s)	4
$(CH_3C_5H_4)_4Ti_4S_4$	5.94 (2 H, m)	
	5.84 (2 H, m)	
	2.08 (3 H, s)	
$[(CH_3)_2CHC_5H_4]_4Ti_4S_4$	5.94 (2 H, m)	
	5.87 (2 H, m)	
	2.75 (1 H, m)	
	1.13 (6 H, d)	

[a] Chemical shifts are quoted relative to internal TMS. [b] Full width at half-height.

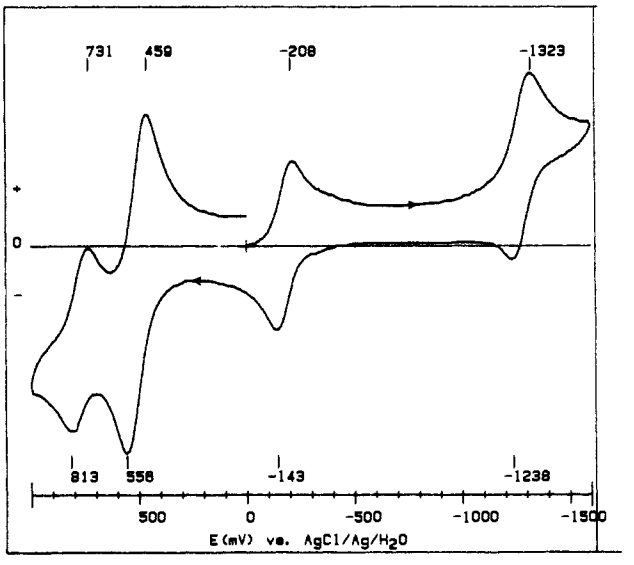

Figure 1. Cyclic voltammogram of $(MeCp)_4V_4S_4$ and Cp_2Fe in CH_2Cl_2 (0.1 M $(Bu_4N)(BF_4)$) vs Ag/AgCl. The wave at 500 mV is due to the Cp_2Fe standard. The sweep rate was 250 mV/s.

Oxidation–Reduction Studies. Cyclic voltammetry experiments on CH_2Cl_2 solutions of **1** show that the cluster can exist in four oxidation states (Figure 1). Each of these oxidation states is interrelated by quasi-reversible couples. The wave centered at −176 mV (vs Ag/AgCl) is assigned as the 0/1− couple on the basis of coulometry. Treatment of CH_2Cl_2 solution of **1** with $[Ph_3C](BF_4)$ gave **[1]**(BF_4) isolated as a black microcrystalline solid. The ^1H NMR signals for **[1]**(BF_4) are clearly isotropically shifted (Table I). It is significant that the isotropic shifts are approximately half those observed in **1**. This salt was further examined by X-ray crystallography. The cluster $(i\text{-}PrCp)_4Ti_4S_4$ shows no reversible electrochemistry in the range ±0.6 V vs Ag/AgCl, but these studies were hampered by the extreme reactivity of **2**.

Structures of $(MeCp)_4V_4S_4$ (1) and $[(MeCp)_4V_4S_4](BF_4)$ ($[1](BF_4)$). The structures of **1** and **[1]**(BF_4) are nearly identical (Figure 2). Each consists of a distorted cube, with vanadium and sulfur atoms occupying alternating vertices. Important bond distances and angles are presented in Table II. Each cluster contains two sets of V–V distance, which differ by only ca. 0.01 Å. The average V–V and V–S distances in **1** and **[1]**(BF_4) differ by only 0.02 and 0.01 Å, respectively. The observed V–V distances are significantly longer than in $(MeCp)_2V_2S_5$[19] (2.658 (1) Å) but

(16) Apparently, the original motivation for revising[15] Dahl's scheme was to explain the paramagnetic ground state of $Cp_4Cr_4O_4$ (Bottomley, F.; Paez, D. E.; White, P. S. *J. Am. Chem. Soc.* **1982**, *104*, 5651) although the ground state may in fact be diamagnetic.[4]

(17) Bolinger, C. M.; Rauchfuss, T. B.; Rheingold, A. L. *J. Am. Chem. Soc.* **1983**, *105*, 6321.

(18) Other compounds characterized in our efforts to prepare $(RCp)_4Ti_4S_4$ include $(RCp)_2Ti_2Cl_4S$ ($^1/_2S$ + $(RCp)TiCl_2(THF)$) and $(RCp)_2Ti_2Cl_2S_5$ (Li_2S_3 + $(RCp)TiCl_3$).

(19) Bolinger, C. M.; Rauchfuss, T. B.; Rheingold, A. L. *Organometallics* **1982**, *1*, 1551.

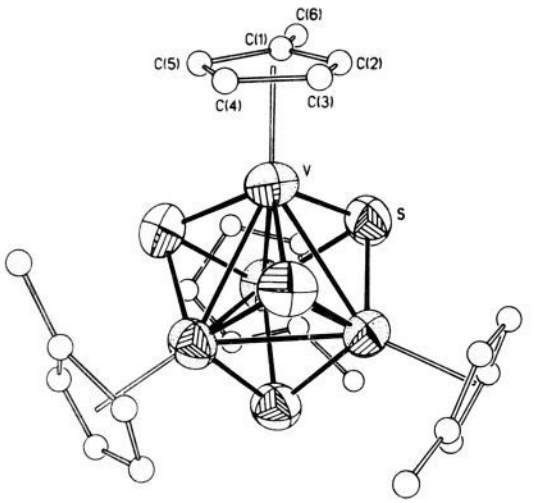

Figure 2. Structure of $(MeCp)_4V_4S_4$ (**1**) and cation of **[1]**(BF_4). The differences between the two clusters are imperceptible.

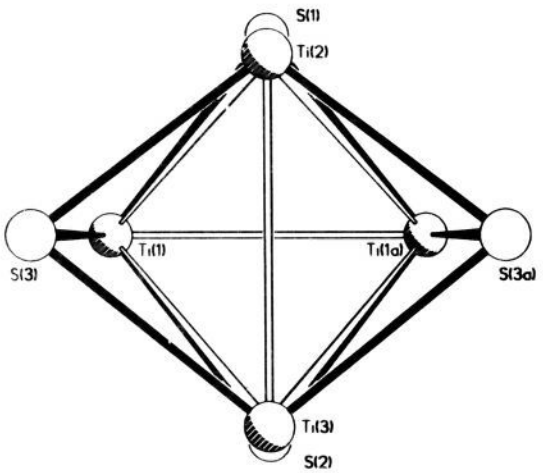

Figure 3. Cubane-like Ti_4S_4 core of $(CH_3C_5H_4)_4Ti_4S_4$ drawn with 40% probability ellipsoids. A crystallographic mirror plane contains S(1), S(2), Ti(2), and Ti(3).

are shorter than the distances found in $[(MeCp)_5V_5S_6]$-$[(TCNQ)_2]$[12] ($V_{ax} - V_{eq}$ = 2.97–3.10 Å and $V_{eq} - V_{eq}$ = 3.21–3.25 Å).[12] The V–V distances observed in the present study are very similar to the intermetallic bonding distances (2.83 Å) in the linear-chain compound VS_4.[20] The V–S–V angles in **1** average 77.5° and are smaller than those in $Cp_4Co_4S_4$[5] (av 96°). This significant structural difference arises because the 72-electron cobalt cluster lacks any Co–Co bonding. The V–S–V angle in **1** as well as the V–V distances in **1** and **[1]**(BF_4) therefore indicate significant metal–metal bonding.

Structure of $(MeCp)_4Ti_4S_4$ (2). In general, the solid-state structure of **2** resembles the vanadium clusters although it does not feature high crystallographic symmetry (Figure 3). The average metal–metal distances in **2** are ca. 0.1 Å longer than in **1** (Table II). On the basis of Shannon's radii for hexacoordinate Ti and V,[21] the difference is predicted to be 0.13 Å in the absence of any electronic effects. The Ti–Ti distances fall into two distinct ranges, giving rise to a D_{2d} distortion of the Ti_4 core. Four Ti–Ti contacts are 3.006 (9) and 3.008 (10) Å, and two are 2.932 (13) and 2.927 (13) Å. These distances are within bonding range on the basis of literature standards.[22,23]

(20) See: Halbert, T. R.; Hutchings, L. L.; Rhodes, R.; Stiefel, E. I. *J. Am. Chem. Soc.* **1986**, *108*, 6437.

(21) Shannon, R. D. *Acta Crystallogr. Sect. A: Cryst. Phys., Diffr., Theor. Gen. Crystallogr.* **1976**, *A32*, 751.

(22) $Cp_6Ti_6O_8$ (Ti–Ti = 2.891 Å): Huffman, J. C.; Stone, J. G.; Krusell, W. C.; Caulton, K. G. *J. Am. Chem. Soc.* **1977**, *99*, 5829. $Cp_5Ti_5S_6$ (Ti–Ti = 3.145 (5)–3.214 (5)): Bottomley, F.; Egharevba, G. O.; White, P. S. *J. Am. Chem. Soc.* **1985**, *107*, 4353.

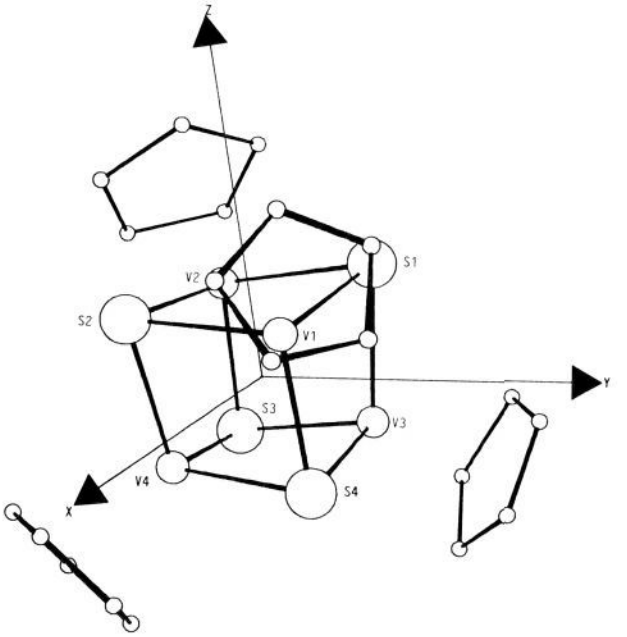

Figure 4. Coordinate axes used in calculations for **1**.

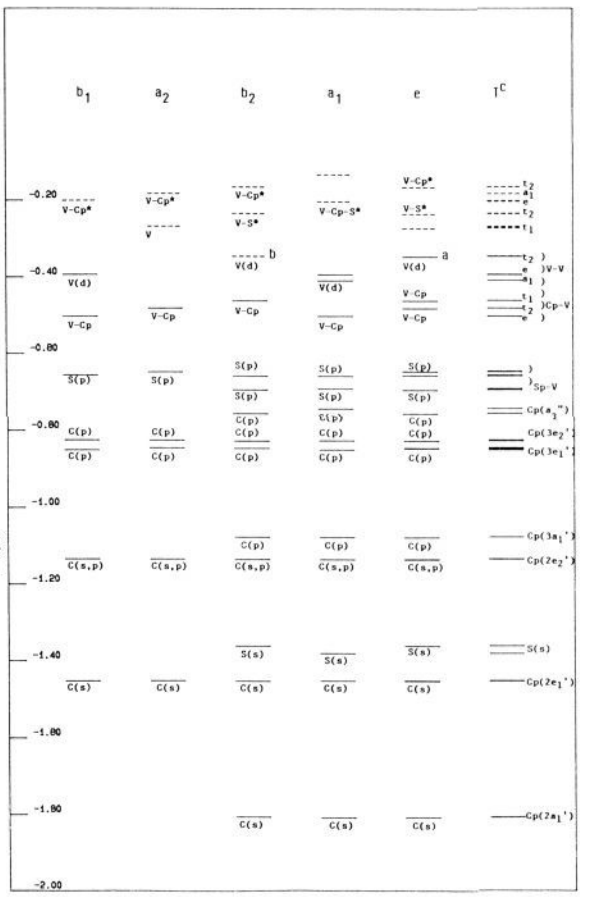

Figure 5. Energy levels for **1** from spin-restricted Xα–scattered wave calculation: (a) HOMO (18e), (b) LUMO ($12b_2$), and (c) the energy levels under T_d symmetry. Dashed lines represent vacant orbitals. The orbitals for each representation are listed in order of increasing energy. Note that there are four accidental degeneracies in the e orbital set.

Spin-Restricted Scattered Wave–Xα Calculations for $Cp_4V_4S_4$. Spin-restricted scattered wave–Xα calculations were performed

(23) The metallic radius for hexagonal titanium is 1.47 Å (Wells, A. F. *Structural Inorganic Chemistry*; Clarendon: Oxford, 1986).

Table II. Selected Bond Distances (Å) and Angles (deg)

	$(MeCp)_4V_4S_4$ (1)	$[(MeCp)_4V_4S_4]BF_4$ ([1](BF$_4$))	$(MeCp)_4Ti_4S_4$ (2)	
		(a) Bond Distances		
M–M(a)	2.884 (3)	2.855 (4)	2.927 (13)	Ti(1)–Ti(1a)
M–M(b)	2.868 (3)	2.852 (5)	3.008 (10)	Ti(1)–Ti(2)
M–M(c)	2.868 (3)	2.855 (4)	3.006 (9)	Ti(1)–Ti(3)
			2.932 (13)	Ti(2)–Ti(3)
M–M(av)	2.873 (3)	2.854 (5)	2.98 (2)	
M–S	2.297 (3)	2.290 (5)	2.356 (9)	Ti(1)–S(1)
			2.399 (10)	Ti(1)–S(2)
M–S(a)	2.293 (3)	2.276 (5)	2.335 (15)	Ti(2)–S(1)
			2.350 (13)	Ti(2)–S(3)
M–S(b)	2.295 (3)	2.285 (5)	2.323 (15)	Ti(3)–S(2)
			2.410 (12)	Ti(3)–S(3)
M–S(av)	2.295 (3)	2.284 (5)	2.36 (2)	
M–C(av)	2.28 (1)	2.25 (3)	2.37 (5)[b]	
M–CENT[a]	1.95 (1)	1.94 (4)	2.04 (6)[b]	
		(b) Bond Angles		
M–S–M(a)	77.8 (1)	77.2 (2)	79.8 (4)	Ti(1)–S(1)–Ti(2)
M–S–M(b)	77.3 (1)	77.3 (2)	76.8 (4)	Ti(1)–S(1)–Ti(1a)
			79.1 (4)	Ti(1)–S(2)–Ti(3)
			75.2 (4)	Ti(1)–S(2)–Ti(1a)
			78.8 (4)	Ti(1)–S(3)–Ti(2)
			77.5 (4)	Ti(1)–S(3)–Ti(3)
			76.0 (4)	Ti(2)–S(3)–Ti(3)
S–M–S(a)	100.7 (1)	101.4 (2)	103.7 (3)	S(1)–Ti(1)–S(2)
S–M–S(b)	101.4 (1)	101.1 (2)	98.1 (4)	S(1)–Ti(1)–S(3)
			99.3 (4)	S(2)–Ti(1)–S(3)
			99.8 (4)	S(1)–Ti(2)–S(3)
			105.2 (7)	S(3)–Ti(2)–S(3a)
			100.9 (4)	S(2)–Ti(3)–S(3)
			101.5 (6)	S(3)–Ti(3)–S(3a)
CENT–M–S	117.3 (5)	115 (1)	116 (2)[b]	CENT–Ti(1)–S(1)
CENT–M–S(a)	117.5 (5)	117 (1)	121 (2)	CENT–Ti(1)–S(2)
CENT–M–S(b)	115.8 (5)	116 (1)	116 (2)	CEnT–Ti(1)–S(3)

[a] CENT = centroid C(1) to C(5). [b] Ti–C distances to ordered ring.

for $Cp_4V_4S_4$ with two sets of atomic sphere radii (Figure 4). The sets differ only in terms of the carbon and hydrogen radii (see the Experimental Section). Both calculations lead to similar results for the orbital energies and charge distributions. In particular, after vanadium–sulfur and vanadium–Cp bonds have been accounted for, the sequences for the remaining 12 "excess" metal orbitals are the same for each set. The results obtained for radii set I are discussed in detail below.

Figure 5 shows the ground-state Xα energy levels. The lowest occupied orbitals at ca. −1.81 and −1.45 Ry are symmetry-adapted combinations of carbon orbitals, corresponding to the $2a_1'$ and $2e_1'$ orbitals, respectively, of the $C_5H_5^-$ ion (1 Ry = 13.61 eV).[24] These are followed by the four sulfur s orbitals at ca. −1.36 Ry and the σ-bonding carbon p–carbon p and carbon p–hydrogen s orbitals of the cyclopentadienyl group between −1.2 and −0.75 Ry corresponding to combinations of $2e_2'$, $3a_1'$, $3e_1'$, $3e_2'$, and a_2'' Cp orbitals.[24] Between −0.65 and −0.7 Ry are found the 12 sulfur p orbital combinations. All the orbitals in this set contain about 20% vanadium character and 40–70% sulfur character. Near −0.5 Ry are several orbitals of principally carbon p_π character corresponding to the e_1'' HOMO of the cyclopentadienyl group again with 20–40% vanadium character. These two groups of orbitals (Figure 5) correspond to vanadium–ligand (Cp and S) orbitals. Above these are the valence orbitals that are principally of vanadium d character (percentage d orbital populations: $7b_1$, 94%; $12a_1$, 90%; $13a_1$, 94%; 18e, 88%). Almost degenerate with the 18e HOMO is the $12b_2$ LUMO, also of principally vanadium d character. The ground electron configuration (tested by transition-state calculation[25]) among these metal orbitals is [... $(12a_1)^2(7b_1)^2(13a_1)^2(18e)^2$]. This overall scheme agrees well with that proposed by Dahl.[8]

The D_{2d} symmetry of the $Cp_4V_4S_4$ molecule is lowered from T_d by the cyclopentadienyl groups while the V_4S_4 core has imposed T_d symmetry in these calculations. Accordingly, there are many near degeneracies in the energy level scheme (Figure 5). The parent T_d representations are indicated on the right-hand side of the orbital energy diagram. In T_d symmetry, the order of the metal–metal bonding orbitals is $a_1 < e < t_2$. The next vacant orbitals (vanadium d) are the metal–metal antibonding orbitals ($t_1 + t_2$) (representation under T_d symmetry). At higher energy still are the metal–metal nonbonding levels ($e + t_1 + t_2$) that are antibonding with respect to the cyclopentadienyl ligand (e_1''; $e + t_1 + t_2$).

Contour plots of the occupied metal–metal bonding orbitals ($12a_1$ (a_1), $7b_1$ (e), and 18 e (t_2)) are illustrated in Figure 6. These plots show the essential vanadium d character of these valence orbitals. The orbitals involved in the vanadium–ligand bonding are primarily the cyclopentadienyl e_1'' (carbon (p)), sulfur (p), and various combinations of vanadium d orbitals ($e + t_1 + t_2$). Figure 7 shows, for example, the occupied $11b_2$ V–Cp–S orbital (percentage total atomic populations: 24% V, 10% S, 59% C).

Spin-Polarized Scattered Wave–Xα Calculation for $Cp_4V_4S_4$. Spin-polarized scattered wave–Xα calculations were carried out for $Cp_4V_4S_4$ with atomic radii set I. These calculations allow differing radial forms for the α and β spin orbitals and lead to an improved description of the ground state in paramagnetic complexes over the restricted method.[26] The α and β spins in such calculations have differing potentials for open-shell configurations that allow for their differing exchange interactions in the molecule. The resultant one-electron energy levels are illustrated in Figure 8. The ground-state configuration for this calculation (tested by transition-state calculation)[25] was found to be $[...7b_1^{\alpha})^1(12a_1^{\alpha})^1(13a_1^{\alpha})^1(12a_1^{\beta})^1(7b_1^{\beta})^1(13a_1^{\beta})^1(18e^{\alpha})^2]$ with the next two vacant spin orbitals $(12b_2^{\alpha})^0(13e^{\beta})^0$. This configuration has an excess of two α spins in the 18e orbital, leading to a net stabilization of α spin orbitals relative to the corresponding β spin orbital due to the greater exchange interactions. This stabilization of the α spin orbitals in $Cp_4V_4S_4$ is only significant for the vanadium-based orbitals, while for the sulfur and cyclo-

(24) Lichtenberger, D. L.; Fenske, R. F. *J. Am. Chem. Soc.* **1976**, *98*, 50.
(25) Slater, J. C. *Adv. Quantum Chem.* **1972**, *6*, 1.
(26) Wood, J. H.; Pratt, G. W. *Phys. Rev.* **1957**, *107*, 995.

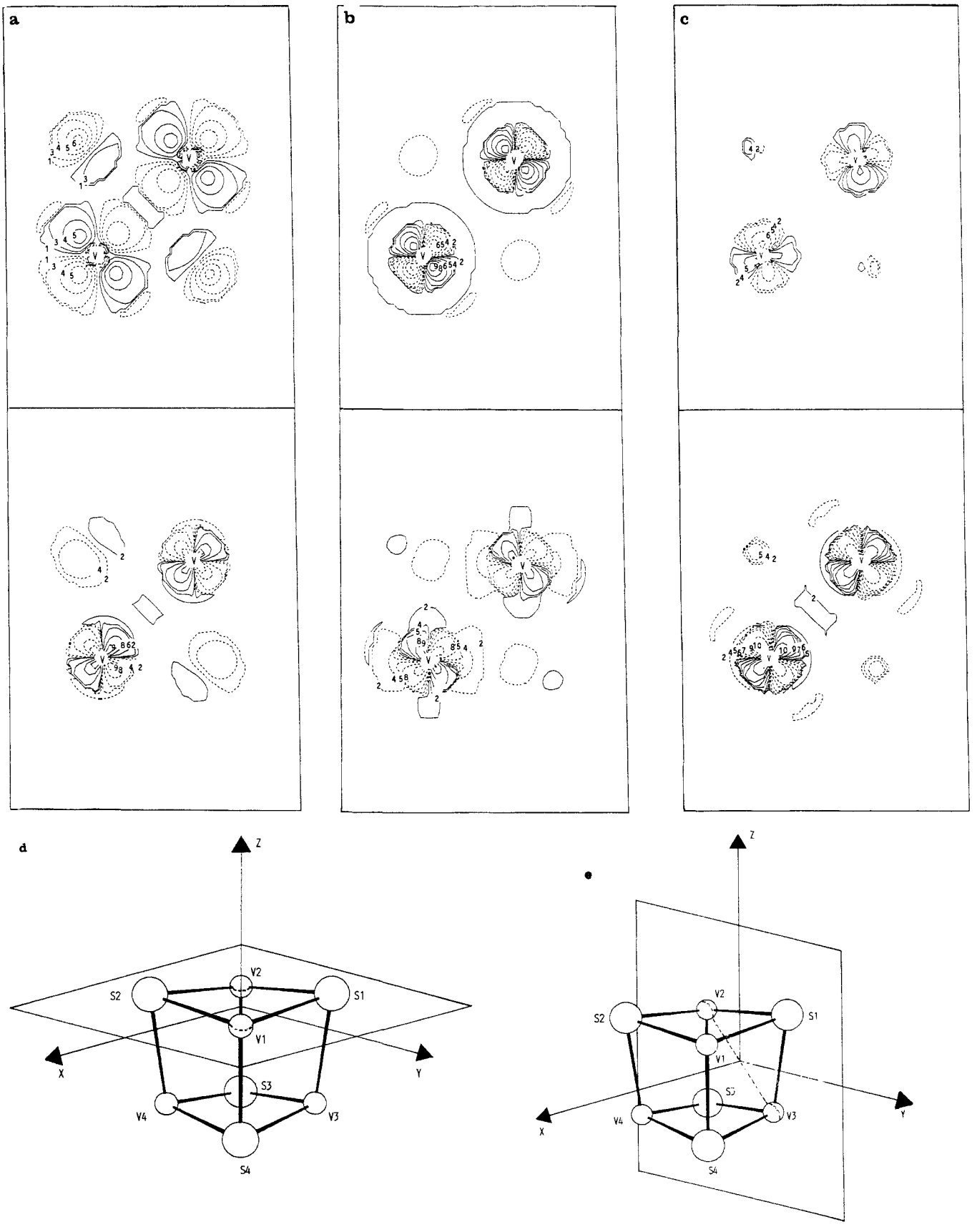

Figure 6. Contour plots of the occupied metal–metal bonding orbitals in $Cp_4V_4S_4$ in the xy and yz planes: (a) $12a_1$ orbital; (b) $7b_1$ orbital; (c) 18e orbital; (d) XY plane (V_1–V_2) at Z = 1.9048 au; (e) YZ plane (V_2–V_3) at X = −1.9265 au. Contours (au): 1, ±0.02; 2, ±0.03; 3, ±0.05; 4, ±0.1; 5, ±0.2; 6, ±0.4; 7, ±0.6; 8, ±0.7; 9, ±0.9; 10, ±1.5. Dashed lines represent negative contour values.

pentadienyl-based orbitals, there is little difference in energy between the α and β orbitals for a particular representation.

The highest occupied orbital, $18e^{\alpha}$, is occupied by the two unpaired α electrons. However, in contrast to the restricted calculation, the lowest unoccupied orbital is now the $12b_2^{\alpha}$ followed by the $18e^{\beta}$ level. The overall charge distribution for the spin-polarized calculation is very similar to that found for the spin-restricted model.

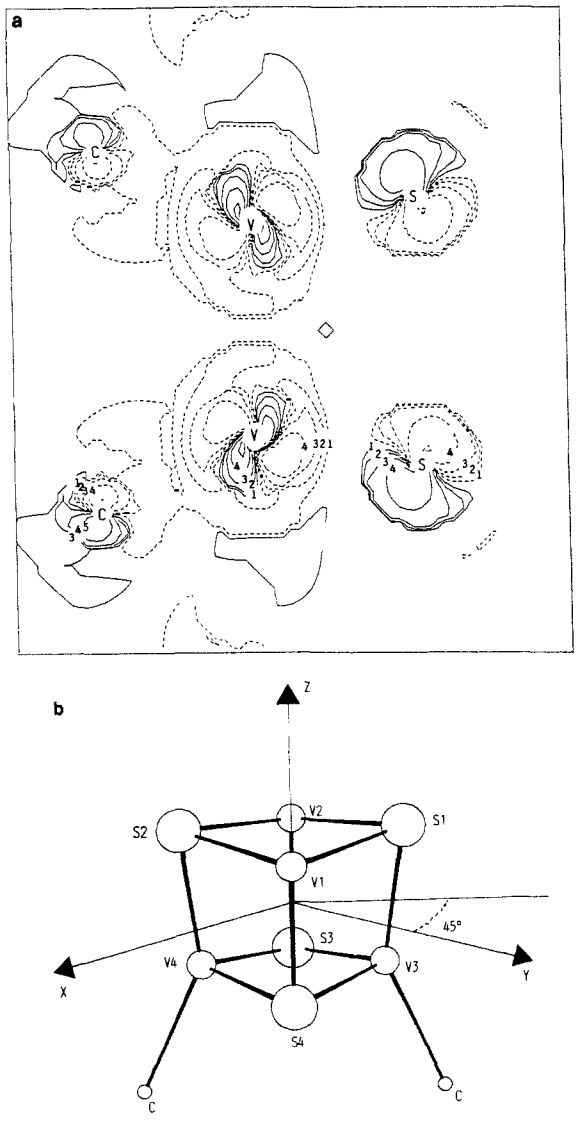

Figure 7. (a) Contour plot of a representative metal–ligand bonding orbital ($11b_2$) in $Cp_4V_4S_4$ in the (b) yz (S_1–S_2–V_3–V_4–C) plane rotated 45° about the z axis. Contours: 1, ±0.02; 2, ±0.05; 3, ±0.1; 4, ±0.2; 5, ±0.4. Dashed lines represent negative contour values.

A spin-polarized calculation for the corresponding monocation $[Cp_4V_4S_4]^+$ was also performed. The occupancy of the orbitals was found to be similar to that for the neutral molecule with a ground-state configuration (tested by transition-state calculations),[25] with a singly occupied 18e orbital corresponding to the removal of a single electron from the HOMO of $Cp_4V_4S_4$.

Discussion

Synthetic and Physicochemical Aspects. The electron-deficient clusters $(RCp)_4V_4S_4$ and $(RCp)_4Ti_4S_4$ were prepared via novel synthetic routes. Some time ago we found that we could desulfurize $(RCp)_2V_2S_4$ to give both **1** and a V_5S_6 cluster.[10,12] This transformation is of interest since it proceeds via the condensation of reactive sulfur-deficient intermediates. This reactivity is somewhat analogous to the condensation of unsaturated metal carbonyls. The other method used for synthesizing **1** is a V_2S_4 + 2V process. The salient feature of this method is that the added Cp_2V units lose Cp fragments under very mild conditions. Other heterocubanes of the type $Cp_4M_2V_2S_4$ can be prepared by this route.[27] A complementary synthetic method involves the addition of metal–metal triple bonds to an M_2S_4 core[4] (eq 2).

$$Cp_2Mo_2(CO)_4 + Cp'_2Mo_2S_4 \xrightarrow[-4CO]{} Cp_2Cp'_2Mo_4S_4 \quad (2)$$

(27) Gammon, S. D.; Rauchfuss, T. B., unpublished results.

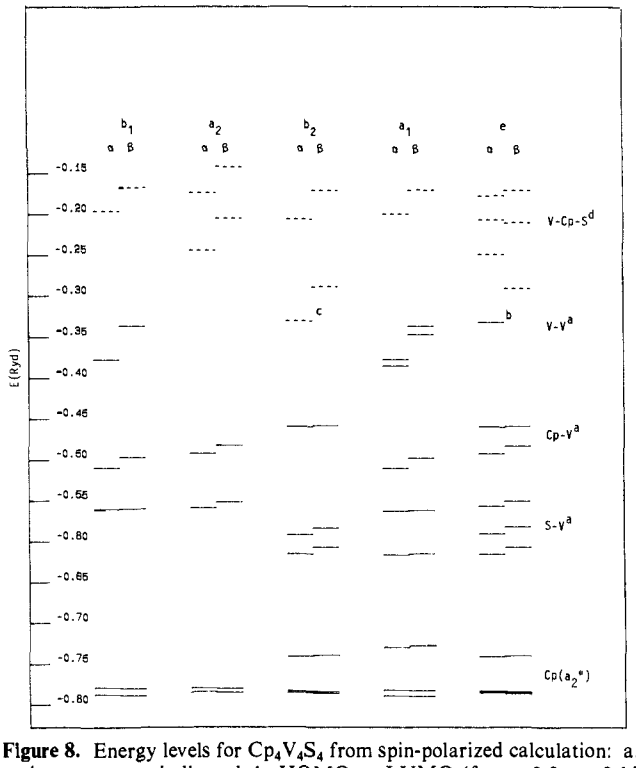

Figure 8. Energy levels for $Cp_4V_4S_4$ from spin-polarized calculation: a, main component indicated; b, HOMO; c, LUMO (from −0.8 to −0.15 Ry). Dashed lines represent vacant orbitals.

The synthesis of $(RCp)_4Ti_4S_4$ illustrates the considerable utility of Si–S reagents in inorganic synthesis.[28] We speculate that the formation of the Ti_4S_4 cubane arises by the condensation of dimers of the formula $(RCp)_2Ti_2S_2(THF)_x$. Conceivably, the 54e cubane $(RCp)_4Ti_2V_2S_4$ could be prepared via a $(RCp)_2Ti_2S_4$ + $(RCp)_2V$ process. It appears, however, that the required $(RCp)_2Ti_2S_4$ would not be stable given that the more electron-rich species $(RCp)_4Ti_4(S_2)_4O_2$ shows no tendency to dissociate.[29]

Compound **1** has a triplet (S = 1) ground state as established by magnetic measurements.[10,11] Its ^1H NMR spectrum also clearly indicates its paramagnetism. The fact that both the ring proton and methyl proton resonances are shifted downfield indicates some dipolar component in the shift mechanism. The direction and magnitude of the downfield-shifted ring proton resonances indicate, however, that the contact term dominates.[30] The fact that the isotropic shifts and peak widths for $[1]^+$ are nearly half those for **1** suggests the same orbital parentage, 18e, for the valence electrons in **1** and $[1]^+$.

The crystallographic analysis establishes that the structures of **1** and $[1]^+$ are virtually identical. The average V–V distance of $[1]^+$ is only 0.022 Å shorter than in **1**. In contrast, the metal–metal distances contract by ca. 0.08 Å in the $Cp_4M_4S_4^{0/+}$ pairs where M = Fe, Co.[5,14] It would therefore appear that the valence electrons in **1** are nealy nonbonding in nature and delocalized over the four V atoms. These observations are in accord with the scattered wave–Xα calculations.

Consistent with the nonbonding character of its HOMO, **1** can function both as an electron acceptor and as electron donor, as determined electrochemically. On the basis of its electrochemistry and its reactivity toward TCNQ,[27] **1** is a noticeably better reducing agent than the 68e cubane $Cp_4Fe_4S_4$. On the other hand, the Ti_4S_4 cluster appears to be very different since it is not oxidizable up to 0.8 V vs AgCl.

(28) Schleich, D. M.; Marti, M. J. *J. Solid State Chem.* **1986**, *64*, 359. Sola, J.; Do, Y.; Berg, J. M.; Holm, R. H. *Inorg. Chem.* **1985**, *24*, 1706. Fenske, D.; Merzweiler, K. *Angew. Chem., Int. Ed. Engl.* **1986**, *25*, 338.
(29) Zank, G. A.; Jones, C. A.; Rauchfuss, T. B.; Rheingold, A. L. *Inorg. Chem.* **1985**, *25*, 1886.
(30) Morse, D. M.; Hendrickson, D. N.; Rauchfuss, T. B.; Wilson, S. R. *Organometallics*, in press.

Bonding. The ground-state configuration for the $Cp_4V_4S_4$ metal–metal bonding orbitals is $12a_1^2 13a_1^2 7b_1^2 18e^2 12b_2$ (under idealized T_d symmetry: $a_1^2e^4t_2^2$). The $12b_2$ orbital is nearly degenerate with the HOMO 18e and is the LUMO ($12b_2^a$) from the spin-polarized calculations. In T_d symmetry this near degeneracy would give an orbitally degenerate $^3T_1$ ground state, which would be Jahn–Teller active. The lowest energy V–V bonding orbital $12a_1$ is not destabilized by V–S antibonding interactions relative to the other V–V bonding orbitals, ($13a_1 + 7b_1$) (e) and ($18e + 12b_2$) (t_2), as has been reported for $Cp_4Cr_4O_4$.[16]

The low-energy portion of the photoelectron spectrum of $(i\text{-}PrCp)_4Mo_4S_4$ suggests the ground-state configuration $a_1^2e^4t_2^6$. The assignments are $^2T_2$ (5.58 eV), ^2E (6.47 eV), and $^2A_1$ (6.9 eV).[7,31] This significant separation between ionizations from the $a_1 + e$ set and the t_2 set suggests that the a_1/e set is more strongly bonding than the t_2. Consistent with this view, oxidation of this Mo_4S_4 cluster leads to very small and irregular decreases in the Mo–Mo distances. The ordering of orbitals calculated for the $[Cp_4V_4S_4]^{n+}$ cluster is in accord with the results on the Mo_4 system. The a_1 and e orbitals are close in energy (−5.10, −5.21 eV) while the t_2 orbital lies at significantly greater energy (−4.49 eV). The similarity of the molecular structures of $Cp_4V_4S_4$ and $[Cp_4V_4S_4]^+$, which differ by one t_2 electron, indicates that the t_2 orbitals are largely nonbonding. Curtis reached a similar conclusion using overlap population analyses in his extended Hückel studies of the $Cp_4M_4S_4$ (M = Cr, Mo) clusters.[4]

The 52e Ti_4 cubane **2** has only four metal-based electrons. Three limiting descriptions of the Ti_4S_4 core are (i) four Ti(III) d^1 centers, which are antiferromagnetically coupled, (ii) a distorted cubane comprised of two two-center, 2e Ti–Ti bonds, and (iii) a fully delocalized cubane. The diamagnetism and short metal–metal distances eliminate the first description. The structural results indicate that a combination of ii and iii more accurately describes **2**. The energy level scheme developed for the near-tetrahedral $Cp_4V_4S_4$ system predicts a paramagnetic ground system for the $Cp_4Ti_4S_4$ molecule. The measured diamagnetism of $Cp_4Ti_4S_4$ and the significant distortion from t_d symmetry of the Ti_4S_4 core to D_{2d} (with two shorter Ti–Ti distances) would suggest that the highest e orbital in the tetrahedral scheme is significantly split ($13a_1 + 7b_1$). In this situation, a ground-state configuration of either $(12a_1)^2(13a_1)^2$ or $(12a_1)^2(7b_1)^2$ would be consistent with the observed diamagnetic ($S = 0$) ground state.

Experimental Section

Materials and Methods. All reactions were performed under an atmosphere of prepurified nitrogen by standard Schlenk techniques. Reagent-grade tetrahydrofuran (THF), hexanes (bp 68–72 °C), and toluene were distilled from Na/K alloy (THF and hexanes) or Na metal (toluene). Dichloromethane was technical grade and was distilled from CaH_2 followed by P_4O_{10}. All other solvents were reagent grade and were dried over 4A molecular sieves. Cp_2V,[32] $Cp_2V_2S_4$,[10] $(MeCp)_2V_2S_4$,[33] and $(Me_3Si)_2S$[34] were prepared by literature methods. Tri-*n*-butylphosphine (Aldrich) was used without purification. $[Ph_3C](BF_4)$ was prepared from Ph_3COH and HBF_4.[35]

Infrared spectra were recorded on a Perkin-Elmer 599B grating instrument. ^1H NMR spectra were recorded on either a Nicolet NT-360 or a Nicolet GE-300 (with internal ^2H frequency lock). Electron-impact (EI) and field-desorption (FD) mass spectra were measured on Varian CH-5 and 731 spectrometers at the University of Illinois Mass Spectrometry Laboratory. Microanalytical data were obtained at the University of Illinois Microanalytical Laboratory.

Reaction of $Cp_2V_2S_4$ with *n*-Bu_3P. Formation of $Cp_4V_4S_4$. Neat *n*-Bu_3P (0.149 mL, 1.95 mmol) was added to a solution of $Cp_2V_2S_4$ (0.301 g, 0.835 mmol) in 10 mL of CH_2Cl_2 at room temperature. After 30 min, the reaction mixture was evaporated to dryness. The residue was washed with hexanes (20 mL) and extracted with 25 mL of CH_2Cl_2 to remove $Cp_5V_5S_6$. The remaining black solid was further purified by Soxhlet extraction with 50 mL of CH_2Cl_2 for 24 h. After the extraction, 0.110 g of $Cp_4V_4S_4$ remained in the thimble. The brown extract was cooled to 0 °C to crystallize 0.067 g of the black crystals. The combined yield was 0.177 g (27%) of $Cp_4V_4S_4$. Electron-impact mass spectrum: *m/e* 592 (M^+), 527 ($M^+ - Cp$), 462 ($M^+ - 2\ Cp$), 397 ($M^+ - 3\ Cp$), 332 ($M^+ - 4\ Cp$). Anal. Calcd for $C_{20}H_{20}S_4V_4$: C, 40.55; H, 3.40; V, 34.40. Found: C, 40.57; H, 3.47; V, 34.23.

Reaction of $(MeCp)_2V_2S_4$ with *n*-Bu_3P. Formation of $(MeCp)_4V_4S_4$. Neat *n*-Bu_3P (0.850 mL, 3.410 mmol) was added to a solution of $(MeCp)_2V_2S_4$ (0.610 g, 1.543 mmol) in 20 mL of CH_2Cl_2. After 1 h, the red solution was evaporated to dryness and the residue extracted with hexanes (5 × 5 mL). The hexanes filtrate was concentrated to 5 mL and cooled to −78 °C. Black crystalline **1** (0.159 g) was isolated by filtration and washed with cold hexanes. The residue from the initial hexanes extraction was sublimed at 150 °C (0.030 mmHg). The sublimate was recrystallized as above to yield additional 0.056 g of the product. Yield: 0.215 g (43%). Electron-impact mass spectrum: *m/e* 648 (M^+), 569 ($M^+ - MeCp$), 490 ($M^+ - 2\ MeCp$), 411 ($M^+ - 3\ MeCp$), 332 ($M^+ - 4\ MeCp$). Anal. Calcd for $C_{24}H_{28}S_4V_4$: C, 44.65; H, 4.35; V, 31.42. Found: C, 44.60; H, 4.44; V, 31.42.

Bulk electrolysis was performed on 4.6 mg of $(MeCp)_4V_4S_4$ in 15 mL of CH_2Cl_2 (0.1 M tetrabutylammonium hexafluorophosphate). Passing current for 48 min through this solution at −600 mV gave 0.85 e/mol of **1** after correcting for background.

Reaction of $(MeCp)_2V_2S_4$ with Cp_2V. Formation of $(MeCp)_2Cp_2V_4S_4$. A solution of Cp_2V (0.200 g, 1.105 mmol) in 15 mL of toluene was added dropwise to a solution of $(MeCp)_2V_2S_4$ (0.214 g, 0.552 mmol) in 20 mL of toluene at −78 °C. The mixture was allowed to warm to room temperature, stirred vigorously for 12 h, and evaporated. The residue was extracted with 20 mL of CH_2Cl_2. Addition of 10 mL of MeOH to the filtrate and gradual concentration of the solution gave 0.26 (76%) black microcrystals. Field desorption mass spectrum: *m/e* 620 (M^+). Anal. Calcd for $C_{22}H_{24}S_4V_4$: C, 42.59; H, 3.90. Found: C, 42.36; H, 3.77.

Reaction of $(MeCp)_4V_4S_4$ with $[Ph_3C](BF_4)$. Formation of $[(MeCp)_4V_4S_4](BF_4)$ ($[1](BF_4)$). A solution of $[Ph_3C](BF_4)$ (0.063 g, 0.190 mmol) in 10 mL of CH_2Cl_2 was added to a solution of **1** (0.122 g, 0.188 mmol) in 10 mL of CH_2Cl_2. The dark red solution immediately turned maroon and was stirred for 1 h. The solution was filtered, concentrated to 10 mL, and diluted with an equal volume of hexanes to crystallize the product. Yield: 0.100 g (72%). Anal. Calcd for $C_{24}H_{28}S_4BF_4V_4$: C, 39.20; H, 3.84. Found: C, 39.00; H, 3.75.

Reaction of $Cp_2V_2S_4$ and $(MeCp)_2V_2S_4$ with *n*-Bu_3P. A solution of $Cp_2V_2S_4$ (0.050 g, 0.139 mmol) in 20 mL of CH_2Cl_2 was added to a solution of $(MeCp)_2V_2S_4$ (0.054 g, 0.139 mmol) in 10 mL of CH_2Cl_2. A solution of *n*-Bu_3P (0.16 mL, 0.643 mmol) in 5 mL of CH_2Cl_2 was then added, and the resulting solution was stirred at room temperature for 1 h. The solvent was removed in vacuo, and the residue was extracted with 10 mL of hexane. The hexane extract was slowly concentrated to about 2 mL to give a black microcrystalline solid. The electron impact mass spectrum of the product showed the following identifiable peaks: *m/e* 648 $[(MeCp)_4V_4S_4]^+$ (95.27%), 634 $[(MeCp)_3CpV_4S_4]^+$ (45.09%), 620 $[(MeCp)_2Cp_2V_4S_4]^+$ (100.00%), 606 $[(MeCp)Cp_3V_4S_4]^+$ (39.21%), 592 $[Cp_4V_4S_4]^+$ (30.89%), 541 $[(MeCp)Cp_2V_4S_4]^+$ (46.09%), 476 $[(MeCp)CpV_4S_4]^+$ (54.84%), 411 $[(MeCp)V_4S_4]^+$ (67.89%), 397 $[CpV_4S_4]^+$ (62.02%), 332 $[V_4S_4]^+$ (85.39%). The intensity of the mass spectral data must be interpreted with caution since the methyl-substituted clusters are somewhat more stable with respect to fragmentation. Furthermore, the extractive workup discriminates against unmethylated cubanes. Most telling in this data is the *m/z* 648:634:620 ratio.

Control Experiments. A solution of $Cp_2V_2S_4$ (0.050 g, 0.139 mmol) in 20 mL of CH_2Cl_2 was added to a solution of $(MeCp)_2V_2S_4$ (0.054 g, 0.139 mmol), stirred for 1 h, and worked up as above. Electron-impact spectrum of the maroon solid product showed only peaks assignable to $[Cp_2V_2S_4]^+$ (*m/e* 360) and $[(MeCp)_2V_2S_4]^+$ (*m/e* 388) and fragments of these units.

A solution of $Cp_4V_4S_4$ (0.0100 g, 0.017 mmol) in 10 mL of CH_2Cl_2 was added to a solution of **1** (0.0109 g, 0.017 mmol) in 10 mL of CH_2Cl_2. The mixture was stirred for 1 h and then evaporated to dryness in vacuo. The EIMS of the residual solid showed fragments for $Cp_4V_4S_4$ and $(MeCp)_4V_4S_4$. No mixed Cp–MeCp clusters were observed.

A 1:1 mixture of $Cp_2V_2S_4$ (0.0061 g, 0.017 mmol) and **1** (0.0109 g, 0.017 mmol) was prepared as above. Electron-impact mass spectrum of the solid residue gave molecular ions for $[Cp_2V_2S_4]^+$ and $[(MeCp)_4V_4S_4]^+$ and their fragments. Mixed Cp–MeCp clusters or dimers were not observed.

A mixture of $Cp_2V_2S_4$ (0.050 g, 0.140 mmol) and $(MeCp)_4V_4S_4$ (0.0901 g, 0.14 mmol) was dissolved in 20 mL of CH_2Cl_2. To this was

(31) Davies, C. E.; Green, J. C.; Stringer, G. H. In *Quantum Chemistry: The Challenge of Transition Metals and Coordination Chemistry*; Veillard, A., Ed.; Riedel: Dusseldorf, 1986; pp 413–424.
(32) King, R. B. *Organometallic Syntheses*; Academic: New York, 1965; p 64.
(33) Darkwa, J.; Giolando, D. M.; Jones, C. A.; Rauchfuss, T. B., submitted for publication in *Inorg. Synth.*
(34) Armitage, D. A.; Clark, M. J.; Sinden, A. W.; Wingfield, J. N.; Abel, E. W.; Louis, E. J. *Inorg. Synth.* **1974**, *15*, 207.
(35) Dauben, H. J.; Honnen, L. R.; Harmon, K. M. *J. Org. Chem.* **1960**, *25*, 1442.

Table III. Crystal and Refinement Data for $(MeCp)_4V_4S_4$ (**1**), $[(MeCp)_4V_4S_4](BF_4)$ ($[\mathbf{1}](BF_4)$), and $(MeCp)_4Ti_4S_4$ (**2**)

	1	$[\mathbf{1}](BF_4)$	**2**
formula	$C_{24}H_{28}S_4V_4$	$C_{24}H_{28}BF_4S_4V_4$	$C_{32}H_{44}S_4Ti_4$
formula wt	648.46	735.26	636.34
cryst syst	cubic	tetragonal	orthorhombic
space gp	$P\bar{4}3n$	$I\bar{4}$	*Cmca*
a, Å	16.551 (3)	10.600 (3)	12.412 (5)
b, Å			17.293 (6)
c, Å		12.600 (3)	24.503 (9)
V, Å^3	4533.8 (16)	1440.8 (7)	5259 (4)
Z	6	2	8
D(calcd), g cm^{-3}	1.425	1.695	1.61
μ(Mo Kα), cm^{-1}	15.4	8.2	15.3
temp, K	295	294	294
cryst size, mm	0.32 × 0.32 × 0.32	0.27 × 0.29 × 0.34	0.22 × 0.36 × 0.41
cryst color	black	black	brown
diffractometer	Nicolet R3m/μ	Nicolet R3m/μ	Nicolet R3m/μ
radiation	Mo Kα	Mo Kα	Mo Kα
wavelength, Å	0.071 073	0.071 073	0.071 073
monochromator	graphite	graphite	graphite
scan method	$\theta/2\theta$	$\theta/2\theta$	$\theta/2\theta$
2θ limits, deg	$4 < 2\theta < 48$	$4 < 2\theta < 44$	$4 < 2\theta\ \theta\ 45$
scan speed, deg min^{-1}	4	var. 5–20	var. 5–20
no. of rflcns collcd	769	560	1944
no. of unique rflcns	671	500	1819
no. of unique rflcns ($F_o > n\sigma(F_o)$)	534 (n = 2.5)	463 (n = 3.0)	558 (n = 3.0)
std rflcns	3 std/97 data (<1% decay)	3 std/97 data (<1% decay)	3 std/97 data (<1% decay)
R(int), %	3.3	2.3	NA
$R(F)$, $R_w(F)$, %	5.31, 5.80	6.40, 6.55	10.5, 12.6
GOF	1.217	1.146	1.91
Δ/σ	0.06	0.01	0.51
$\Delta(\rho)$, e Å^{-3}	0.60	0.68	0.50
N_o/N_v	7.1	5.9	5.6

added a solution of PBu_3 (0.070 mL, 0.280 mmol) in 5 mL of CH_2Cl_2, and it was stirred at room temperature for 1 h. After removal of the solvent, the ^{1}H NMR of the residue was recorded. The products were identified as $(MeCp)_4V_4S_4$ (unreacted starting material) and $Cp_4V_4S_4$ (56.5 ppm).

Synthesis of (*i*-PrCp)TiCl$_3$. A mixture of $(i\text{-PrCp})_2TiCl_2$ (18 g) and $TiCl_4$ (13 mL) in a dry 500-mL glass tube was vacuum sealed. After it was heated at 120 °C for 60 h, the tube was cooled and opened under an inert atmosphere. The orange-brown solid obtained was washed with hexanes to remove unreacted $TiCl_4$ and vacuum dried. The solid was sublimed at 60 °C (0.03 mm) to give 18.2 g orange crystalline (*i*-PrCp)$TiCl_3$. Anal. Calcd for $C_8H_{11}Cl_3Ti$: C, 36.75; H, 4.24, Cl, 40.68. Found: C, 37.01; H, 4.21; Cl, 40.48. ^{1}H NMR ($CDCl_3$): 6.90 (m), 3.25 (m), 1.35 (d) ppm.

Synthesis of (RCp)$_4$Ti$_4$S$_4$ (R = CH$_3$, *i*-Pr). In a typical experiment, $[(MeCp)TiCl_2(THF)]_x$[36] (1.20 g, 6.06 mmol) was prepared in THF (30 mL) from (MeCp)$TiCl_3$ and Zn according to Green's method.[37] To this green solution was added $(Me_3Si)_2S$ (1.45 mL, 6.06 mmol). The solution turned red-brown immediately and was stirred for 18 h, after which the solvent was removed in vacuo. The dark brown residue was extracted with hot hexanes (100 mL). The filtrate was concentrated to about 10 mL and cooled to −25 °C overnight to give brown-black microcrystalline $(MeCp)_4Ti_4S_4$. The yields were ≳60%. Anal. Calcd for $C_{24}H_{28}S_4Ti_4$: C, 45.30; H, 4.44; S, 20.16. Found: C, 44.79; H, 4.39; S, 19.95. Analysis for Cl showed only a trace. Theoretical C and H analyses should be 45.12 and 4.36, respectively, since ^{1}H NMR spectroscopy showed that approximately 4.6% of the cyclopentadienyl ligands are unsubstituted (C_5H_5 resonance at 5.73 ppm). Electron-impact mass spectrum: *m/e* 636 (M^+) (22.90%); 622 ($M^+ - CH_2$) (1.53%); 557 ($M^+ - CH_3C_5H_4$) (2.73%); 478 ($M^+ - 2\ CH_3C_5H_4$) (5.73%); 399 ($M^+ - 3\ CH_3C_5H_4$) (4.91%); 320 ($M^+ - 4\ CH_3C_5H_4$) (3.63%).

The procedure for $(i\text{-PrCp})_4Ti_4S_4$ was as above with (*i*-PrCp)$TiCl_3$. Anal. Calcd for $C_{32}H_{44}S_4Ti_4$: C, 51.35; H, 5.92. Found: C, 51.98; H, 6.11. Electron-impact mass spectrum: *m/e* 748 (M^+) (100%).

X-ray Crystallographic Structure Determinations. Crystals of **1** and its BF_4 salt suitable for diffraction experiments were obtained by recrystallization from hexanes and CH_2Cl_2/hexanes (2:1) at room temperature, respectively. Preliminary photographic characterization revealed *m3m* and 4/*m* Laue symmetries for **1** and $[\mathbf{1}](BF_4)$. Systematic absences in the diffraction data limited the choices of space groups for **1** to $P\bar{4}3n$ and $Pm\bar{3}n$ and for $[\mathbf{1}](BF_4)$ to $I4$, $I\bar{4}$, $I\bar{4}/m$, and $I4/m$. The expected presence of approximate tetrahedral cluster geometry and the apparent values of Z suggested that the V_4S_4 clusters were located at $\bar{4}$ sites. This led to an initial selection of $P\bar{4}3n$ and $I\bar{4}$ as the space groups for **1** and $[\mathbf{1}](BF_4)$. These selections were confirmed by the chemically reasonable and computationally stable solutions and refinements of these structures. Crystal and refinement data are summarized in Table III.

Unit cell parameters were obtained from the least-squares fit of the angular settings of 25 reflections (**1**, $22° < 2\theta < 29°$; $[\mathbf{1}](BF_4)$, $17° < 2\theta < 23°$). Intensity data were collected to the 2θ limits of availability. No corrections for absorption were required for either structure (uniform crystal dimensions, low absorption coefficients, and T_{max}/T_{min} values of 1.13 for **1** and 1.22 for **2**).

The structures of **1** and $[\mathbf{1}](BF_4)$ were solved by direct methods, which provided the V and S atom locations. In the final refinement, all nonhydrogen atoms were anisotropic, and all hydrogen atoms were idealized and updated (d(C–H) = 0.96 Å). In $[\mathbf{1}](BF_4)$, constraint of the B–F distance to 1.34 (1) Å was imposed. The presence of unusually large thermal coefficients for B, F, and the methyl–C atoms for $[\mathbf{1}](BF_4)$ reveals the presence of high-thermal motion and/or disorder in the anion and methyl group; no alternative F atom positions were found in dif-

Table IV. Atomic Coordinates (×10^4) and Isotropic Thermal Parameters (Å^2 × 10^3)

	x	*y*	*z*	*U*[a]
		$(MeCp)_4V_4S_4$		
V	5553 (1)	9327 (1)	8109 (1)	39 (1)*
S	4174 (2)	9323 (2)	8263 (2)	42 (1)*
C(1)	6677 (8)	8538 (10)	8259 (10)	71 (6)*
C(2)	6667 (8)	9059 (9)	8902 (10)	75 (6)*
C(3)	5957 (9)	8921 (8)	9356 (9)	70 (5)*
C(4)	5561 (9)	8291 (9)	9000 (7)	64 (5)*
C(5)	5996 (10)	8037 (8)	8319 (8)	68 (5)*
C(6)	5777 (13)	7352 (9)	7774 (10)	119 (9)*
		$[(MeCp)_4V_4S_4](BF_4)$		
V	6195 (3)	618 (2)	1712 (2)	69 (1)*
S	4225 (4)	1475 (4)	1526 (3)	75 (1)*
B	0	5000	2500	505 (101)*
F	209 (46)	3974 (22)	2009 (24)	414 (22)
C(1)	7149 (43)	2349 (30)	1008 (37)	149 (18)*
C(2)	6791 (28)	1677 (42)	302 (29)	127 (13)*
C(3)	7246 (41)	637 (40)	157 (27)	152 (17)*
C(4)	8121 (26)	477 (33)	1015 (32)	132 (14)*
C(5)	8121 (49)	1491 (72)	1581 (26)	264 (31)*
C(6)	6593 (52)	3575 (41)	1258 (44)	365 (41)*
		$(MeCp)_4Ti_4S_4$		
Ti(1)	1179 (5)	1088 (3)	1279 (2)	107 (2)*
Ti(2)	0	2370 (5)	1854 (4)	150 (7)
Ti(3)	0	2325 (5)	658 (3)	107 (4)*
S(1)	0	1044 (7)	2032 (4)	102 (5)*
S(2)	0	999 (7)	506 (4)	149 (8)*
S(3)	1504 (9)	2450 (5)	1275 (5)	149 (5)*
C(1)	1914 (25)	−101 (16)	1164 (14)	214 (19)
C(2)	2062	103	1721	134 (12)
C(3)	2828	711	1743	206 (17)
C(4)	3154	883	1201	193 (17)
C(5)	2588	381	843	175 (16)
C(6)	1443 (48)	−705 (34)	901 (19)	247 (24)
C(7)	477 (43)	3640 (27)	2210 (18)	84 (16)
C(8)	1308 (54)	3190 (37)	2299 (25)	162 (32)
C(9)	965 (33)	2738 (26)	2698 (17)	61 (13)
C(10)	0	2479 (25)	2833 (19)	116 (17)
C(11)	0	3116 (31)	2546 (24)	181 (23)
C(12)	0	4198 (46)	1849 (32)	231 (34)
C(13)	731 (50)	2598 (25)	−229 (17)	70 (16)
C(14)	948 (30)	3238 (17)	52 (13)	140 (13)
C(15)	0	3534 (27)	230 (21)	30 (14)
C(16)	0	2967 (39)	−137 (27)	77 (23)
C(17)	662 (55)	3769 (33)	442 (24)	129 (24)
C(18)	0	2232 (50)	−486 (41)	163 (43)
C(19)	0	4363 (35)	457 (39)	154 (42)

[a] Asterisk indicates equivalent isotropic U defined as one-third of the trace of the orthogonalized U_{ij} tensor.

(36) Gamborota, S.; Floriani, C.; Chiesi-Villa, A.; Guastini, C. *J. Am. Chem. Soc.* **1983**, *105*, 7295.
(37) Lucas, C. R.; Green, M. L. H. *Inorg. Synth.* **1976**, *16*, 237.

Table V. Parameters Used in Scattered Wave–Xα Calculations (Set I)

atom	coordinates, au			radius,[a] au
OUT I	0.0	0.0	0.0	9.5541*
V	−1.9265	−1.9265	1.9048	2.3899
S	−2.3619	2.3619	2.3863	2.4444
C(1)	3.1570	3.1570	5.8497	1.6789*
C(2)	2.2800	5.2866	4.5838	1.6787*
C(3)	3.8668	5.7250	2.5356	1.6792*
H(1)	2.2999	2.2999	7.5842	1.3009*
H(2)	6.4449	0.5917	5.1199	1.3005*
H(3)	−3.6809	7.2984	−1.1241	1.3031*

[a] Asterisk indicates set II radii, OUT II; 9.201, C; 1.60, H; 0.95 au. α values V; 0.725 56, S; 0.724 75, C; 0.759 28, H; 0.777 25, OUT (set I); 0.754 61, OUT (set II); 0.754 61.

ference maps. The enantiomorphs reported each represent the hand that produced a value of 1.0 (1) for a $\Delta f''$ multiplicative factor on η refinement.

All samples of **2** examined diffracted very weakly with broad peak widths (>1° at half-height). Preliminary photographic characterization revealed *mmm* Laue symmetry, and systematic absences in the diffraction data indicated the orthorhombic space groups of either *Cmca* or *C2cb* (nonstandard *Ab2a*). *E* value statistics suggested the centrosymmetric alternative ($|E^2 - 1| = 0.96$); trial refinements of a full Ti_4S_4 skeleton in *C2cb* led to fatal correlation phenomena for those atoms symmetry related in *Cmca*. In *Cmca*, Ti(2), Ti(3), S(1), and S(2) reside on a mirror plane. Data were collected to the 2θ units of availability and were not corrected for absorption ($T_{max}/T_{min} = 1.07$).

The structure was solved by direct methods. The η^5-$CH_3C_5H_4$ rings on Ti(2) and Ti(3) are disordered about the mirror plane and were only partially resolved as multiple concentric rings with variously populated CH_3 positions. The η^5-$C_5H_4CH_3$ ring on Ti(1) is ordered and was constrained to a rigid, pentagonal geometry (d(C–C) = 1.420 Å) to conserve data. Only the Ti and S atoms were anisotropically refined. No attempt was made to incorporate hydrogen atom contributions.

Atomic coordinates for **1**, [**1**](BF_4), and **2** are given in Table IV. All computations used the SHELXTL program package (Nicolet Corp., Madison, WI).

Computational Details. The electronic structure of $[(C_5H_5)_4V_4S_4]$ was calculated by the SCF–scattered wave–Xα method[38,39] with the program XASW of Case and Cook.[40] The geometric structure of the molecule was adapted from the X-ray crystal structure $[(CH_3C_5H_4)_4V_4S_4]$ such that all vanadium and sulfur atoms were exactly equivalent; i.e., T_d symmetry was imposed on the V_4S_4 core. The overall symmetry of the idealized molecule is D_{2d}. The starting molecular potential was constructed from a superposition of neutral-atom charge densities with overlapping atomic spheres.[41] The atomic sphere radii were chosen either by the method of Norman[42] as the atomic number radii reduced by a factor of 0.88 (I) or with the same radii of vanadium and sulfur as I but with reduced radii for carbon and hydrogen as used for planar aromatic[43,44] molecules (II) (Table V). The partial wave expansion was taken to $l = 2$ for the vanadium atom, $l = 1$ for the sulfur and carbon atoms, and $l = 0$ for hydrogen atoms. The α values used were taken as those reported by Schwarz.[45] The calculations were continued until the maximum relative charge in the potential at all points in the molecule was less than 10^{-3}. Spin-restricted calculations were performed for both sets I and II, and a spin-polarized calculation was performed for set I. A Watson sphere[46] of charge −1 and radius equal to that of the outer sphere was used for calculations on the analogous $[Cp_4V_4S_4]^+$ cation. The charge distributions were calculated by the charge partitioning method of Case, Cook, and Karplus.[47,48]

Acknowledgment. This research was supported by the National Science Foundation (to T.B.R.). Partial support was also provided by the donors of the Petroleum Research Fund, administered by the American Chemical Society.

Registry No. 1, 93347-79-6; [**1**](BF_4), 111237-34-4; **2**, 111237-35-5; $Cp_4V_4S_4$, 111237-36-6; $(MeCp)_2Cp_2V_4S_4$, 111237-37-7; $(MeCp)_3CpV_4S_4$, 111266-89-8; $(MeCp)Cp_3V_4S_4$, 111237-38-8; $(i\text{-}PrCp)_4Ti_4S_4$, 111237-39-9; $Cp_2V_2S_4$, 111266-88-7; $(i\text{-}PrCp)TiCl_3$, 69276-78-4; $(MeCp)_2V_2S_4$, 87174-39-8; $(i\text{-}PrCp)_2TiCl_2$, 12130-65-3; $(MeCp)TiCl_2(THF)_{1.5}$, 111237-42-4; $(Me_3Si)_2S$, 3385-94-2; Cp_2V, 1277-47-0; $[Ph_3C](BF_4)$, 341-02-6; $TiCl_4$, 7550-45-0.

Supplementary Material Available: Tables of bond angles and distances, isotropic and anisotropic thermal parameters for **1**, [**1**](BF_4), and **2**, and scattered wave–Xα orbital energies and orbital populations for $Cp_4V_4S_4$ (14 pages); tables of observed and calculated structure factors (11 pages). Ordering information is given on any current masthead page.

(38) Johnson, K. H. *Adv. Quantum Chem.* **1973**, *7*, 143.
(39) Case, D. A. *Annu. Rev. Phys. Chem.* **1982**, *33*, 151.
(40) Cook, M.; Case, D. A. *Program XASW Version 2*, personal communication.
(41) Herman, F.; Williams, A. R.; Johnson, K. H. *J. Chem. Phys.* **1974**, *61*, 3508.
(42) Norman, J. G., Jr. *J. Chem. Phys.* **1974**, *61*, 4630.
(43) Case, D. A.; Cook, M.; Karplus, M. *J. Chem. Phys.* **1980**, *73*, 3294.
(44) Case, D. A.; Karplus, M. *J. Am. Chem. Soc.* **1977**, *77*, 6182.
(45) Schwarz, K. *Phys. Rev. B: Solid State* **1971**, *B5*, 2466.
(46) Watson, R. E. *Phys. Rev.* **1958**, *111*, 1108.
(47) Case, D. A.; Karplus, M. *Chem. Phys. Lett.* **1976**, *39*, 33.
(48) Cook, M.; Karplus, M. *J. Chem. Phys.* **1980**, *72*, 7.